

# MEMS 30μm-thick W-band Waveguide Switch

Z. Baghchehsaraei<sup>1</sup>, U. Shah, S. Dudorov, G. Stemme,  
J. Oberhammer  
Microsystem Technology Laboratory, EE School  
KTH Royal Institute of Technology  
Stockholm, Sweden  
<sup>1</sup>zargham@kth.se

Jan Åberg  
MicroComp Nordic  
Friparksvägen 3, 146 38  
Tullinge, Sweden  
jan.aberg@microcomp-nordic.se

**Abstract**—This paper presents for the first time a novel concept of a MEMS waveguide switch based on a reconfigurable surface, whose working principle is to short-circuit or to allow for free propagation of the electrical field lines of the TE10 mode of a WR-12 rectangular waveguide. This transmissive surface is only 30μm thick and consists of up to 1260 reconfiguring cantilevers in the waveguide cross-section, which are moved simultaneously by integrated MEMS comb-drive actuators. For the first fabrication run, the yield of these reconfigurable elements on the chips was 80-86%, which still was good enough for resulting in a measured insertion loss in the open state of better than 1dB and an isolation of better than 20dB for the best designs, very wideband from 62 to 75GHz. For 100% fabrication yield, HFSS simulations predict that an insertion loss in the open state of better than 0.1dB and an isolation of better than 30dB in the closed state are possible for designs with 800 and more contact points for this novel waveguide switch concept.

**RF MEMS; reconfigurable surface; waveguide switch**

## I. INTRODUCTION

Traditionally, there are two methods used for rectangular waveguide switches at high frequencies. Either rotary electrical motor is utilized to make or break the waveguide path [1], [2] or a p-i-n diode is incorporated inside the waveguide acting as switch [3], [4]. Motors are heavy and bulky in comparison to p-i-n diodes, which, however, exhibit poor RF performance.

A third method is to incorporate RF microelectromechanical (MEMS) switching devices in the waveguide. This method benefits from general advantages of RF MEMS switches such as good RF performance and small size.

To the knowledge of the authors, the Ku- and K-band waveguide switch presented by M. Daneshmand et al. [5] is the only publication using MEMS for waveguide switching. MEMS thermally plastic deformable actuators have been integrated with a ridge waveguide to construct the switch. For this switch, a return loss of better than 15 dB, insertion loss of 1-2.8 dB and an isolation of better than 15 dB was achieved.

In this paper, we introduce a novel RF MEMS waveguide switch utilizing up to 630 reconfigurable elements for shortcircuiting the electric field lines of the TE10 mode of a waveguide cross-section. The MEMS waveguide switch is only 30 μm thick, supported by a 500 μm substrate. Combination of

vertical *contact cantilevers* is used to switch ON or OFF the wave propagation in the waveguide. This method provides advantages of rectangular waveguides such as low insertion loss and high power handling capabilities, combined with advantages of electrostatically actuated MEMS, including low waveguide loss, good RF switching performance (in

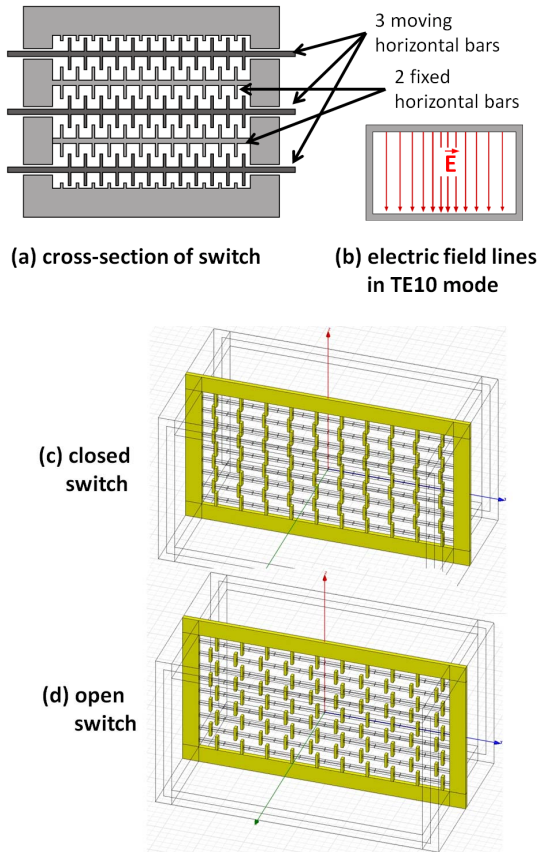


Fig. 1 Concept of novel MEMS waveguide switch: (a) cross-section of switch drawn for 3 moving and 2 fixed horizontal bars and 20 cantilever columns (resulting in 120 contact points; for comparison, design D with 11 moving and 10 fixed horizontal bars, and 30 cantilever columns consists of 1260 contacts); (b) electric field lines in TE10 mode to be short-circuited by the reconfigurable surface; (c) OFF state (closed) and (d) ON state (open) of the waveguide switch.

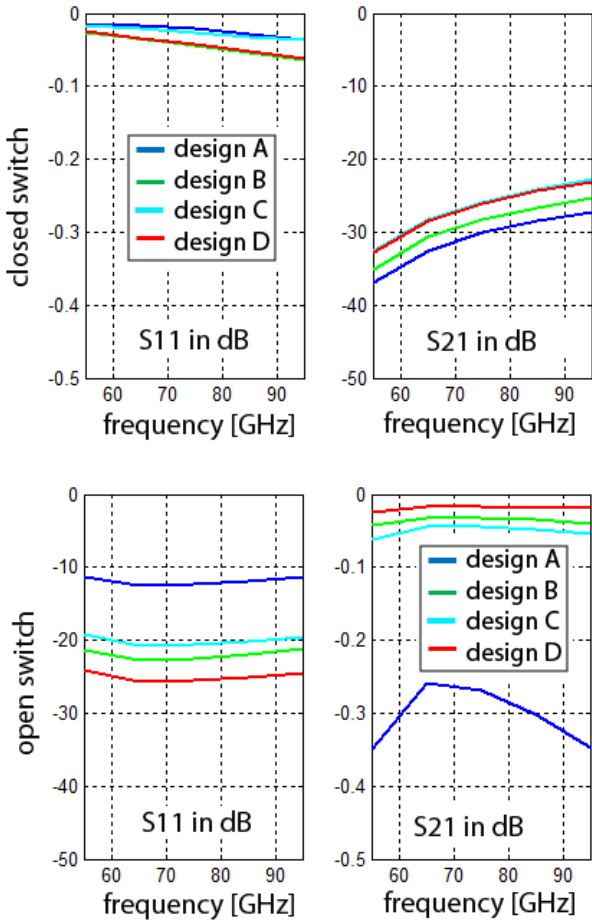


Fig. 2 HFSS simulation result for the implemented designs A-D.

comparison to p-i-n diodes) and drastically miniaturized size (in comparison to bulky rotary motors).

## II. CONCEPT AND DESIGN

Fig. 1 shows a schematic of the proposed MEMS waveguide switch in both ON and OFF states. The reconfigurable surface is implemented in a WR-12 rectangular waveguide ( $3.099\text{ mm} \times 1.549\text{ mm}$ ) and consists of two sets of micromachined vertical *contact cantilevers* separated every other line in the horizontal direction as shown in Fig. 1a. The first set of contact cantilevers is fixated and the second set is movable synchronously in the horizontal direction. When the switch is in the ON state, shown in Fig. 1d, there is a gap between the first and second set of cantilevers which allows the wave to propagate freely through the reconfigurable surface. When the switch is in the OFF state, shown in Fig. 1c, the movable set of contact cantilevers are laterally moved by external MEMS actuators to short-circuit the electric field lines of the predominant TE10 mode (Fig. 1b). In this case the wave propagation is blocked.

The contact cantilevers are distributed uniformly in the waveguide. The number of contact cantilevers can be optimized for achieving good RF performance both in ON and OFF states, as a large number of vertical cantilevers increases

the off-state isolation but also affects the on-state insertion loss negatively. For the present designs, the width and thickness of the contact cantilevers are  $5\text{ }\mu\text{m}$  and  $30\text{ }\mu\text{m}$ , respectively. The overlap between the contact cantilevers in the closed state is  $5\text{ }\mu\text{m}$ . Fig. 2 shows the simulation results for four different designs whose parameters are summarized in Table I.

MEMS electrostatic comb drive actuators with folded beam springs are placed outside the waveguide wall to move the contact cantilevers. The design is based on push-pull actuators and it is required to displace the contact cantilevers  $12\text{ }\mu\text{m}$  in opposite directions to achieve open (ON) or closed (OFF) states. COMSOL Multiphysics simulation resulted in design of three different actuators with spring constants of  $2.21\text{ N/m}$ ,  $4.36\text{ N/m}$ ,  $7.83\text{ N/m}$  and nominal actuation voltages of  $50\text{V}$ ,  $71\text{V}$  and  $90\text{V}$ , respectively.

Microscope photographs and a SEM picture of a fabricated chip are shown in Fig. 3. Movable contact cantilevers are connected to a shuttle by the use of vertical bars and a grid

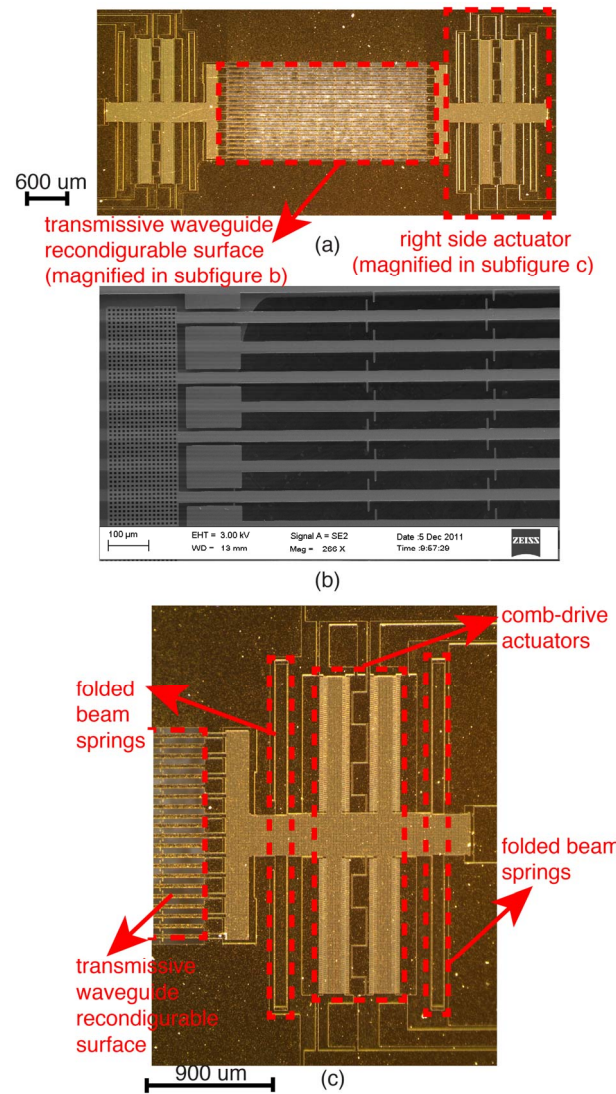


Fig. 3 Image of a fabricated device: (a) microscope image of full chip including the waveguide reconfigurable surface in the middle and the MEMS actuators at the sides; (b) SEM image of magnified part of central reconfigurable surface; (c) microscope image of MEMS actuators on the right side of the waveguide reconfigurable surface including four folded beam springs and two stages of comb-drive actuators.

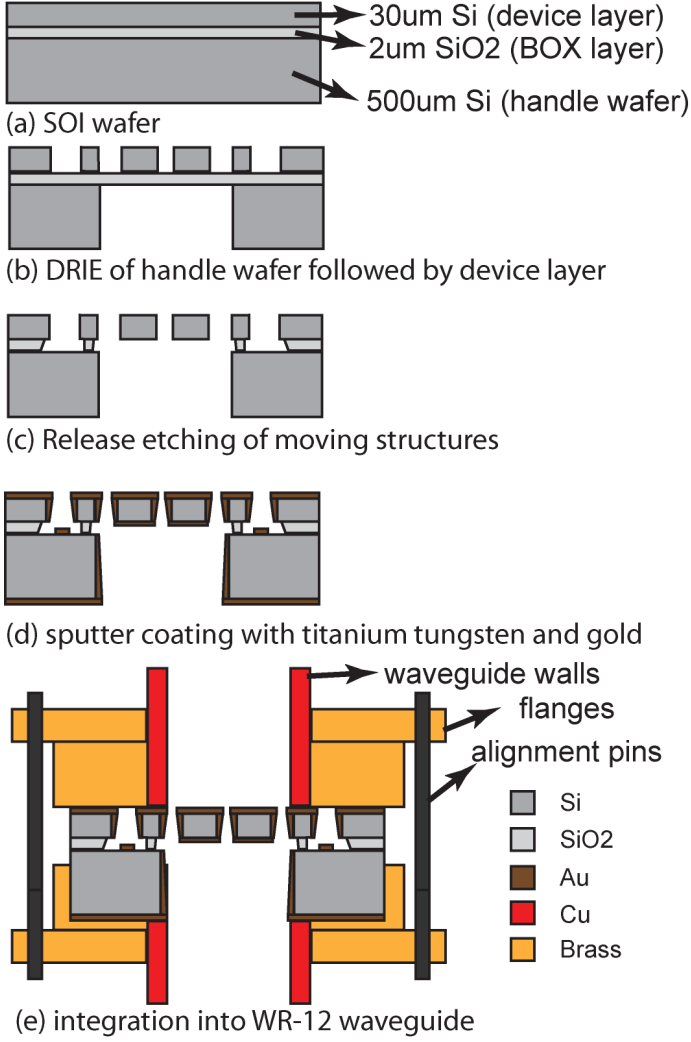


Fig. 4 Basic process flow of MEMS waveguide switch: (a) SOI wafer; (b) deep reactive ion etching of the handle wafer and device layer, (c) followed by release etching of the moving structures and putting the chips in critical point drier; (d) sputter coating with titanium tungsten and gold; (e) integration of the chip into a waveguide section.

structure parallel to the narrow wall of the waveguide. Applying voltage to the comb drives displaces the whole shuttle, which results in the displacement of the structure in direction parallel to the wider wall of the waveguide and which reconfigures the cantilever contacts.

### III. FABRICATION AND WAVEGUIDE INTEGRATION

The micromachining process flow of the waveguide switch, fabricated in an SOI RF MEMS process developed by the authors [6], and an additional back-etching process of the handle wafer, is summarized in Fig. 4.

A special section of a WR-12 rectangular waveguide flange, shown in Fig. 4e, is fabricated for integrating the chips into the waveguide. The chip is fixated in a recess of a bottom waveguide flange and a conducting polymer sheet is applied on

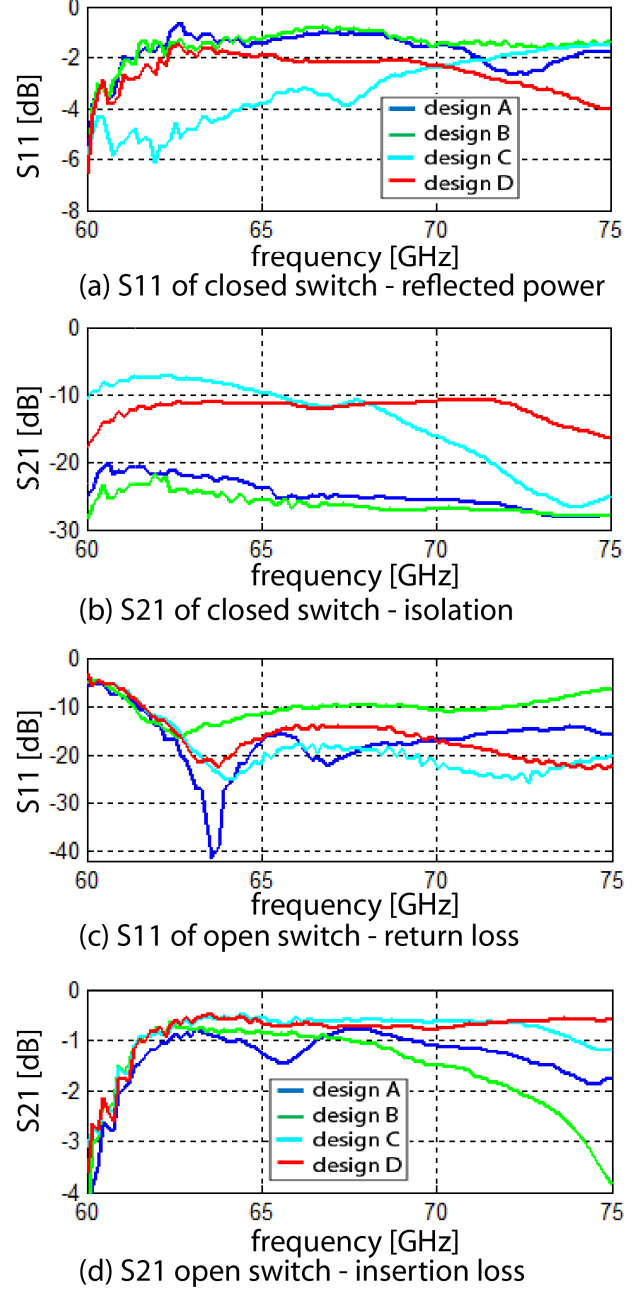


Fig. 5 S-parameter measurement results of different MEMS waveguide switches of designs A-D.

the front side of the chip before closing the top flange for providing good electrical conductivity and thus low loss.

### IV. MEASUREMENT RESULTS

For providing good isolation in the closed state, the most important design parameter is the number and distribution of vertical bars shortcircuiting the electrical field lines in the TE10-mode. The denser the bars, the more the wave propagation is blocked. The numbers of vertical bars is 20 for design A and B, and 30 bars for design C and D. The

simulation results shown in Fig. 2 confirm the expectation that C and D are blocking the wave propagation better than A and B.

For the open state, however, in addition to the number of vertical bars, the distribution and number of gaps are important which is defined by the number of horizontal bars. The more distant the bars from each other the less fraction of the travelling wave is reflected. Consequently, it is anticipated that design A with 9 horizontal bars causes the least return loss, followed by design C with 17 bars. Design B and D both have 21 horizontal bars but design B with less number of contact points has lower return loss in comparison to design D with more gap in the structure. Simulation results of Fig. 2 shows that both return loss and insertion loss are expected to be best for design D, followed by B and C, and the worst for A.

Fig. 5 shows the RF measurement results of prototypes of the four designs, whose performance in comparison to the expectations from the simulation results is compromised by the poor fabrication yield (Table I). In the open-switch state, the measured insertion loss (Fig. 5d) is better than 1dB for major part of the measured frequency range (60-75GHz) for the designs C and D, and better than 2dB but less consistent for the designs A and B. The measured return loss of the open-switch state (Fig. 5c) is better than 15dB loss for designs A, C and D, and better than 10dB for most of the frequency band but less consistent for design B. In the closed-switch state, the measured isolation (Fig. 5b) is better than 20dB for designs A and B, and still better than 10dB for design D which is performing much worse, but very inconsistent for design C. The measured reflected power in the open-switch state (Fig. 5a) is between 1dB and 2dB for most of the spectrum for designs A and B, between 2dB and 3dB for most spectrum for design D, but very inconsistent for design C.

In general, the measured results of these novel waveguide switches show that the fabricated prototypes are clearly able to block the propagation for the closed state, and to allow transmission to a high degree for the open state. However, the measurement results are not as good as expected from simulation. The discrepancy between the simulation and measured results is mainly due to the yield which inhibits complete shortcircuiting of the field lines in the closed state. Table I summarizes the total number of contact points for each design and the estimated yield of these very first fabricated prototype devices. It is anticipated that devices with higher yield of cantilevers surviving the fabrication process will result in much better switch performance.

Unfortunately, the MEMS comb-drive actuator did not sufficiently actuate for the expected (simulated) actuation voltages of 50 V due to excessive lateral overetching. Therefore, for measuring these samples, devices which are fixated mechanically in the on or off-states were utilized.

## V. CONCLUSION

This paper reported on design, fabrication and evaluation of a novel concept of a MEMS waveguide switch based on a reconfigurable transmissive surface of a thickness of only 30 $\mu$ m, consisting of up to 630 simultaneously reconfigurable cantilevers and 1260 electrical contact points. Even with a poor fabrication yield of the first prototypes of the reconfigurable surfaces of only 80-86% for the very first prototypes presented in this paper, the open-state insertion loss is better than 1dB and the off-state isolation is better than 20 dB for the best designs and 62-75 GHz band. Simulations of a complete device, including losses, predict on-state insertion loss and off-state isolation of less than 0.1dB and better than 25dB, respectively, of this novel, extremely miniaturized waveguide switch concept.

TABLE I  
SUMMARY OF DIFFERENT DESIGNS

Design	No. of horizontal bars	No. of vertical bars	Total contact points	Estimated yield
A	9	20	360	83%
B	21	20	840	86%
C	17	30	1020	80%
D	21	30	1260	86%

## ACKNOWLEDGMENT

The research leading to these results has partly been funded from the European Community's Seventh Framework Programme under grant agreement n° 267528 (xMEMS, grant holder: Göran Stemme).

## REFERENCES

- [1] R. Kich, M. N. Ando, "Compact waveguide "T" switch," U.S. Patent 6 201 906 B1, March 13, 2001.
- [2] Dow-Key Microwave Corporation, Ventura, California, USA. <http://www.dowkey.com>
- [3] R. Henry, M. Heitzmann, G. Sillard, "PIN diode switch mounted in a ridge waveguide," U.S. Patent 4 660 008, Apr. 21, 1987.
- [4] G. F. Craven, "Waveguide switch," U.S. Patent 3 979 703, Sept. 7, 1977.
- [5] M. Daneshmand, R. R. Mansour, N. Sarkar, "RF MEMS waveguide switch," *IEEE Trans. Microwave Theory & Tech.*, vol. 52, no. 12, pp. 2651-2657, December 2004.
- [6] M. Sterner, N. Roxhed, G. Stemme, J. Oberhammer, "Static Zero-Power-Consumption Coplanar Waveguide Embedded DC-to-RF Metal-Contact MEMS Switches in Two-Port and Three-Port Configuration," *IEEE Trans. on Electron Devices*, vol. 57, no. 7, pp. 1659-1669, July 2010.